Journal of Thermal Analysis and Calorimetry, Vol. 80 (2005) 271–283

FORMS OF VIBRATIONS AND STRUCTURAL CHANGES IN LIQUID STATE

B. Hlaváček[1*], *J. Šesták*[2], *L. Koudelka*[3], *P. Mošner*[3] *and J. J. Mareš*[2]

[1]Department of Polymers, University of Pardubice, Čs. Legií 565, 532 10 Pardubice, Czech Republic
[2]Institute of Physics, Academy of Sciences, Cukrovarnická 10, 162 53 Prague 6, Czech Republic
[3]Department of General and Inorganic Chemistry, University of Pardubice, Čs. Legií 565, 532 10 Pardubice, Czech Republic

The forms of vibrations and displacements of particles in amorphous structures have been investigated. The particles, moving on highly non-linear amplitude, are responsible for the creation of disordered structures of amorphous bodies. The non-linear oscillators, even if 'few' in concentration, are characterized by unpredictable trajectories in phase space. The non-linear oscillators are fully developed in the liquid state above the crossover temperature T_{cr} and between T_{cr} and T_g their number decreases. Under T_g they completely disappear. The interconnection between the linear oscillators in blocks plays the most important role in the characteristic time spectra in liquid state. Using the additive properties of elements polarizibilities, the number of acoustical units in individual blocks at T_{cr} is estimated to be about 600 units. The diameter of blocks at T_{cr} was estimated to be about 1.8 nm. Even if the non-linear high amplitude motions disappear at solidification, the remnants of structural irregularity remain and the disordered structure of glass is formed.

Keywords: *crossover temperature, deterministic chaos, glass transition, non-linear oscillators, solid–liquid transition*

Introduction

Substantial fluctuations of liquid density in the area of critical temperature T_c appear as observable phenomena visible to naked eye [1]. The facts that liquid phase under critical temperature is divided into solid-like structures and voids filled up with gas-like molecules (the so called 'wanderers'), has been well known for a long time [2]. Some of the modern structural theories (so-called mode coupling theory, MCT) describing the structural phenomena of liquid state at lower temperatures are also based on a similar idea of local density fluctuation as well [3]. The assumption of heterogeneity in liquid phase goes back to assumption of semi-crystalline phase by Kauzman [4], as well as to the assumptions of coexistence of gas liquid semi-structures related to numerous works of Cohen *et al*. [5–11].

Model structure

In this study we take also the liquid structure as a mechanically divided structure formed by blocks (domains, or clusters) on one side, and the individual 'semi-evaporated' units, which are subjected to non-linear anharmonic motions of high amplitudes, on the other side. It is assumed that the highly non-linear oscillators maintain the individual character of their motions and are taken, in the present study, as simple individual units about a monomer size [12]. On the other hand, the blocks are assumed to possess interconnected microstructure and are composed of identical elastically bonded particles packed to the high (density) level reaching the density of van der Waals liquid phase (Fig. 1).

The blocks are characterized by a module, which reaches the level of glassy state and keeps the swarm of particles in one block together. A dynamical equilibrium exists between the block particles and the semi-evaporated particles, as well as between the semi-evaporated particles and the gas phase. The existence of randomly distributed, random size molecular clusters in a viscous liquid has been discussed since 1959 till present days [5–11, 13]. Loosely packed regions separate these clusters. Here we consider that the inter-clusters regions contain molecules whose vibrations are strongly anharmonic, giving rise to non-deterministic vibration movements.

The blocks and their inter-blocks bonding structure form the main contributing factor responsible for dynamical parameters, such as the viscosity or bulk elasticity of liquid sample. The blocks are also responsible for complex relaxation effects, because the interconnected linear oscillators forming their structures interact. On the other hand, the 'semi-evaporated' particles acting as the non-linear oscillators are

* Author for correspondence: borek.hlavacek@upce.cz

1388–6150/$20.00

Akadémiai Kiadó, Budapest, Hungary
Springer, Dordrecht, The Netherlands

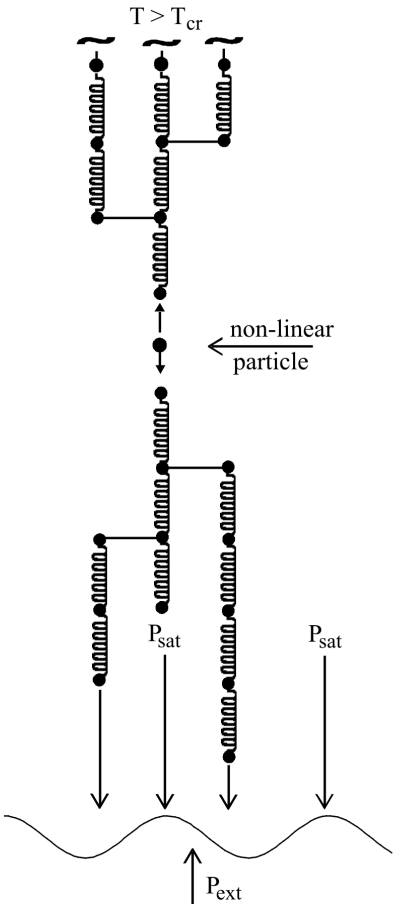

Fig. 1 Schematic model for solid-like structure just above the T_g temperature, when the first particle starts to act as non-linear oscillator and causes irregularity in structure of linear elements. The separation of blocks causes interference with α process, which forms the infinite structural network

responsible for erratic character of Brownian motion displacements in liquids [14]. The 'semi-evaporated' particles are acting against the external pressure and exercise a 'push aside' effect on the individual blocks in their vicinity. The opening thus created (Fig. 2) through straightforward amplitude jump, can be directed to any direction in amorphous phase. The non-linear oscillators of semi-evaporated particles can perform their oscillations on several different amplitudes [15, 16], and their motions carry with them elements of uncertainty described most cases by the non-linear, non-deterministic theories [17–25] of chaos. Because the initial positional coordinates of such non-linear oscillator for its subsequent position and momentum cannot be determined in advance, the differential changes in initial conditions will bring completely different trajectories. The general rule for the non-deterministic chaos theories [17–25] is consequently reflected into the structure of amorphous body in glassy state, which depends on the way of cooling and will have the irregular character.

For the displacement of block as a whole, the maximum retardation time will show the level of interconnections inside of block structure, characteristic of a given block size, which changes with temperature (Fig. 3). It is assumed that the block size, together with maximum block retardation time τ_{max}, decreases with increasing temperature. The block disintegrates as the critical temperature is approached [15, 16]. In the opposite case, the blocks bind themselves to a rigid structure as the temperature decreases below T_{cr}.

The amplitudes of vibration movements below the critical temperature

Under the critical temperature T_c we consider the following most important marking points, as the characteristic temperatures for amorphous body, regarding the vibration amplitudes size:

- the boiling point temperature T_b,
- the crossover temperature T_{cr},
- the transition temperature of glassy state T_g,
- Vogel's temperature T_v.

It can be stated: $T_c \geq T_b \geq T_{cr} \geq T_g \geq T_v$ (the model proposed has the following distinct characteristics of vibration modes at different temperatures or temperature areas, which should be mentioned and pinpointed beforehand for the text to be clearer).

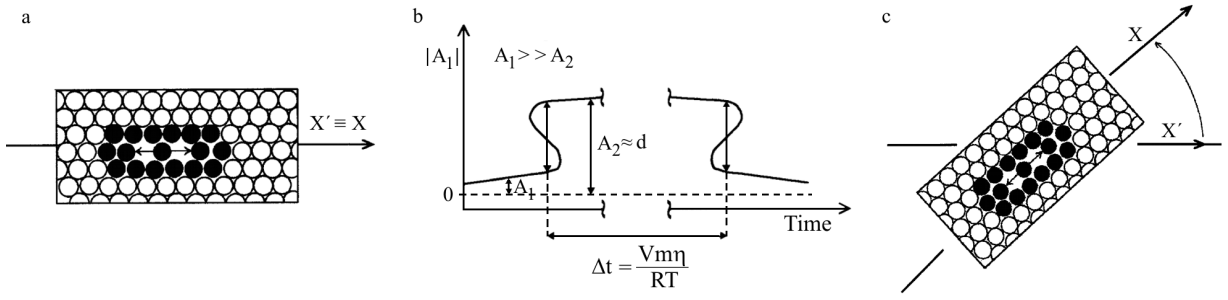

Fig. 2 Sudden amplitude jump of non-linear particle (a), (b) can be performed in any direction (case 'c') in the sample space

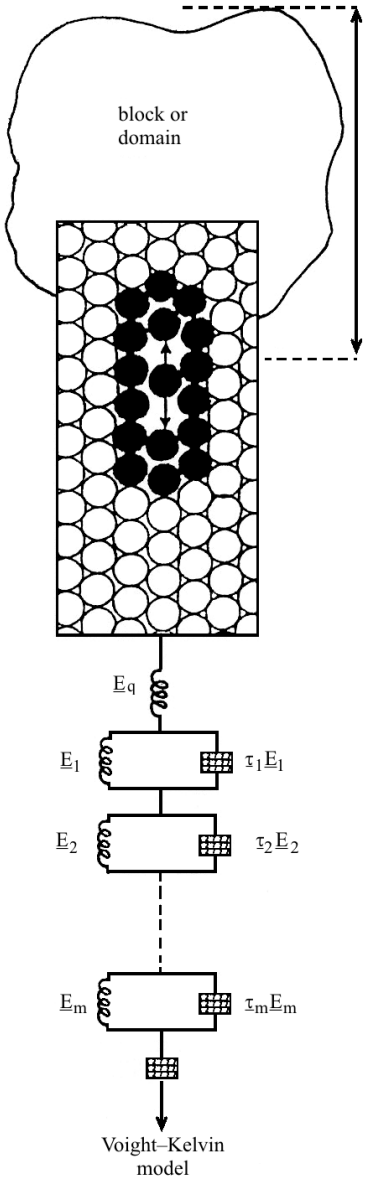

Fig. 3 Schematic picture for a liquid-like structure where the linear elements represented in blocks by Voigt series are not connected through the elastic network and are mobile, being restricted in their mobility by balance of saturation pressure P_{sat} and by the external pressure P_{ext} only (Fig. 1). The blocks are a source of cooperative phenomena of sample time response

The bottom part of van der Waals curve on the liquid side plays the important role for the evaluation of non-linear amplitude size.

The onset of the spinodal part of van der Waals curve seems to pose a sensible restrain on the upper amplitude of vibration motion. This limit, if exceeded has to lead to vacancy enlargement in which the particles in vicinity of high-amplitude oscillator have to take away the vibration energy of particle, by their own avalanche like displacement. This type of energy withdrawal from high amplitude vibrating particle can only be performed successfully by particles in vicinity below the liquid point T_b, without the destruction of the sample through the creation of a gas phase in the sample bulk.

The level of bottom of van der Waals curve for isothermal case can be found easily for small volumes by looking for the intercept of spinodal curve [26] with the low volume of van der Waals dependence. The intercept point is at volume fraction of 0.385 of critical volume. At boiling point T_b, the non-linear movement stops for some semi-evaporated particles, as the bond of particle to a 'strange' attractor of Lorenz type [23, 24] enlarges its basin of attraction and is eventually interrupted as the particle leaves the oscillatory movement for a gas phase. Between the crossover temperature and the boiling point, the high amplitudes of vibration are able to mechanically perturb the original bonding of blocks to such a level, that shear module disappears. In contrast to behavior of material at this higher temperature zone, below the crossover temperature, the substantial rise in shear module G contributes (as a new element) to limitation in vacancy enlargement, as the sample is able to store the elastic energy W connected to shear module [27], inside of the vacancy space:

$$W = 8\pi G r_0 (r_1 - r_0)^2 \quad (1)$$

The radius r_0 represents the radius of a rigid sphere approximating the particle, and r_1 is approximating the size of radius of the cavity. For example the cavity of size $r_1=2r_0$ formed in solid with modulus G of about $G=10^{10}$ N m^{-2} needs about 125 kJ mol^{-1} [27], while in liquids of van der Waals–Eyring's type, such level of internal void expansion inside of bulk of liquid sample, leads to Trouton's rule [2].

The non-zero shear module below the T_{cr} has drastic impact on vacancy size and on the sizes of maximal diffusion jumps, which are depressed or eliminated as the temperature decreases. The presence of inter-block bonding will bring the shear module to the non-zero level and the elastic network will be formed. The fact of different ways of inter-block bonding has basic influence also on the fragility phenomena's [28, 29]. Above the crossover temperature the diffusion process, is driven mainly by few particles, out of the block area's, which are undergoing the amplitudes switch. Thus the relation formed by product of viscosity, size of the diffusing particle and diffusion coefficient, divided by absolute temperature and Boltzmann's constant [30, 31] cannot retain its form below T_{cr}. The most apparent impact of shear module can be demonstrated on the temperature dependence of the alpha α and beta β relaxation processes. (Also this topic will be treated more closely in the following text). In T_g vicinity the changes in vibration amplitudes of average vibrations can be also demonstrated by the experimental measurements of Debye–Waller factor [32].

Earliest experimental justification of the structural heterogeneity of liquids

X-ray diffraction

The X-ray diffraction studies are the oldest methods supporting the existence of dual structure in bulk of liquids [33]. These studies have shown that for a liquid, even above its boiling point, the coordination number (characterizing the number of particles in the closest vicinity) falls drastically in the area of temperatures between boiling point and T_c, but the distance characteristic of the first peak of radial distribution $g^{\bullet}(r)$ of particles in vicinity hardly changes as the temperature approaches the critical temperature region. On the other hand, the experimental proof of compact structure, expressed through unchanged radial distribution $g^{\bullet}(r)$, implies the existence of voids and cavities filled with 'semi-evaporated' particles, to make up for the overall volume of the sample characterized by average density.

The characteristic of local heterogeneity using the positron annihilation spectroscopy

The volumes of vacancies are exactly determined and are reported in numerous papers on positron annihilation spectroscopy PASCA [34–38] (Fig. 4). The experiments of PASCA provide the unusually high coefficients of thermal expansion in the vacancy area. The volumes of vacancies are very sensitive to temperature changes above the glassy transition and to the external pressure changes in the boiling point area. In the present study, the vacancies in liquid state contain the semi-evaporated particles without which the transition from bulk of sample to gas phase at boiling point would not be possible. As can be seen from the data of Fig. 4 the coefficient of thermal expansion in vacancies areas is about ten to a hundred times as high as that in the block areas. At temperatures $T \le T_g$ (for the amorphous bodies and the whole piece of sample) the coefficient of thermal expansion is $\alpha_1 \approx 1 \cdot 10^{-4}$ K^{-1}. At temperatures $T \ge T_g$ the coefficient of thermal expansion is $\alpha_2 = 4.1 \cdot 10^{-4}$ K^{-1}. The PASCA readings at crossover temperature are higher than $\alpha_{V,1} \approx 4 \cdot 10^{-3}$ K^{-1}. The discontinuity in properties for liquid structure is apparent. It could be contemplated that the liquid contains locally expanding spots, which bear a responsibility for the high coefficient of thermal expansion of liquids in general.

Three types of entropy contributions

The entropy contribution connected with the semi-evaporated state (Fig. 2), which is created inside the liquid system in vacancies areas, can potentially be contemplated as well [15, 16]. For the temperatures $T \le T_g$ the entropy S main contributions can be explained as:

$$S \cong k_B [\ln W_{th} + \ln W_{conf}] \quad (2)$$

and for $T \ge T_g$

$$S \cong k_B [\ln W_{th} + \ln W_{conf} + \ln W_{semievap}] \quad (3)$$

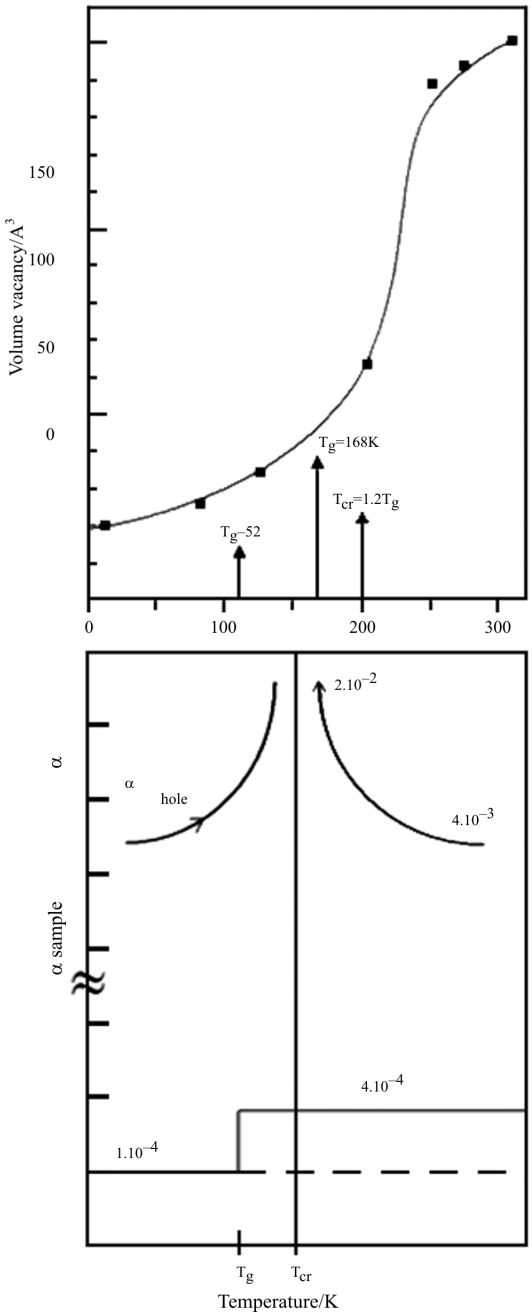

Fig. 4 a – The stepwise rise of vacancy volume in the vicinity of T_g=168 K for polybutadiene; the data provided by Bartoš *et al.* [19] are gratefully acknowledged, b – The coefficient of volumetric thermal expansion calculated from Fig. 4a, for the vacancies, and the data of α approximately taken from literature [43, 60] quoted for the sample at glassy state

This type of entropy changes composed of three distinct contributions, viz. thermal, conformational and highly non-linear, has been experimentally confirmed in recent works of Johari [39, 40]. Because the vacancies areas, thanks to the reports on PASCA experiments, have well defined size (which is larger than the van der Waals volume, but smaller than is the 0.385 fraction of critical volume of the particles involved), we can estimate the change in enthalpy connected with the semi-evaporated state. As has been shown by Hirschfelder *et al*. [2], the whole amount of evaporation enthalpy is needed to produce an expansion of cavity to level of twice as high as is the particle diameter. So to produce a cavity of size about 0.385 of fraction of critical volume, a proportionally smaller part of evaporation enthalpy ΔH_{evap} can be used, as the first estimate for the energy of void creation. The assumption of the $\Delta H_{semievap}=\Delta H_{evap}/n$, where n is about 2–4 or even higher, will be in agreement with the PASCA experiments as well as with the estimate on viscosity by Eyring *et al*. [41, 42].

The basic phase space behavior of semi-evaporated particles – highly non-linear oscillator

The equation of motion for particle vibrations

The equation of vibration motion for non-linear oscillations of 'n^{th}' particle is:

$$m_n \frac{\delta^2 \xi}{\delta t^2} + \frac{\delta U_n}{\delta \xi} = F_{ext,n} \tag{4}$$

where the oscillator external force $F_{ext,n}(t)$ is created through action of many particles in the vicinity, and m_n is the particle mass, comparable in size with dimensions of acoustical unit [12] of about monomer size. U_n is the potential energy characteristic of the potential valley in which the n^{th} vibration acoustical unit is performing its oscillations. The term $\xi=r-r_{0,n}$ is the deviation from the bottom of local potential valley.

The vibrations of particle take place inside of the potential valley $U_n(t)$ of the n^{th} oscillator:

$$U_n(t) = U_{0n}\left(r_{0,n}(t)\right) + \\ + \frac{1}{2} f_n^{\otimes}\left(r_{0,n}(t)\right)\xi^2 - \frac{1}{3} g_n\left(r_{0n}(t)\right)\xi^3 \tag{5}$$

where in the first approximation the individual parameters U_{0n}, $f_n^{\otimes}$, g_n, $r_{0,n}$ for the block's particles are constant and time-independent and vary smoothly with temperature only; $r_{0,n}$ is a vector pointing to the bottom of potential valley of the n^{th} oscillator. The term U_{0n} stands for the basic level of internal energy, $f_n^{\otimes}$, g_n are characteristic parameters of local potential valley, which depend on positions of particles in the closest vicinity. The equation of motion for particles in the form of Eq. (4) is the same for block particles as for the semi-evaporated particles. However, if Eq. (5) is substituted into Eq. (4), great differences will appear in the solutions obtained between the individual cases for $g_n\to 0$, $r_{0,n}(t)$=const. (the case of ideal solids) or for $g_n\neq 0$ (the case of real solids or liquids) or when $g_n(t)$, $f_n^{\otimes}(t)$, $U_{0n}(t)$ vary with time. The last example represents the structural changes in solids and the diffusion or flow onset for liquids.

Beside Eq. (4) in variables ξ and t an additional equation for description of $r_{0,n}(t)$ development in time (for the bottom well displacements) would be needed.

The mathematical treatment of strong non-linearity for one oscillator above T_g transition

To find fast solution to Eq. (4) and provide illustrative examples that can be easily visualized, the second-order differential Eq. (4) is usually turned into two separate first-order differential equations. This procedure is performed in the deterministic chaos theories [17–25] as well as in studies of 'organized structures' or in studies of non-equilibrium thermodynamics [21, 22].

By choosing the variables $A_1\equiv\xi$ and $A_2\equiv d\xi/dt$ we can rewrite Eq. (4) into (two first order differential equations) the following forms [15, 16]:

$$\frac{dA_1}{dt} = \alpha_{11}A_1 + \alpha_{12}A_2 \tag{6}$$

$$\frac{dA_2}{dt} = \alpha_{21}A_1 + \alpha_{22}A_2 \tag{7}$$

Equations (6) and (7) can be analyzed further in the vicinity of vibration stationary point. The system of Eqs (6) and (7) will have non-zero solution only if

$$\det\begin{vmatrix} \alpha_{11}-\lambda & \alpha_{12} \\ \alpha_{21} & \alpha_{22}-\lambda \end{vmatrix} = 0 = \lambda^2 + a_1\lambda + a_2 = 0 \tag{8}$$

where $a_1=\alpha_{11}+\alpha_{11}$, $\alpha_2=\alpha_{11}\alpha_{22}-\alpha_{12}\alpha_{21}$.

The changes from a solid to a liquid state, as well as the other higher temperature transitions, can be investigated through the change of parameters a_1 and a_2 within a certain range as shown in our previous communication [15, 16].

The mathematical reasoning gives the basis to the existence of vacancies, which stems from the considerations of high non-linearity of Eqs (4–8), suggesting the particle trajectories have a non-deterministic character. At solidification process, the end points of the trajectories in phase space are aiming at

different spots, which forms the irregular structure of the glassy state. The scheme for the amplitude development for two coordinates ξ_n, $d\xi_n/dt$ for different temperatures in phase space is shown in [15, 16]. Following such line of perception, the higher transitions such as the boiling or critical point can be considered too. The fraction of vacancies can roughly be estimated through the density changes for the liquid sample [15]. While only few vacancies exist at lower temperatures (according to Bueche [43] the ratio of vacancies to vibrating particles is equal to 1:40 at T_g), at the critical temperature the amount of vacancies reaches the level at which the condensed phase disintegrates completely [15, 16] and all oscillating particles are able to reach the upper vibration amplitude with addition of very tiny amount of energy.

The linear cooperative phenomena in blocks

As a result of separation of the non-linear effects from the linear blocks areas, some more than half-century-old experimental results and mathematical techniques can successfully be used for the investigation of very topical time phenomena in liquid–solid transitions (following the temperature interval between T_V and T_{cr}). The new physical explanations about certain phenomena, nowadays intensively studied [13, 44–56], connected with α and β processes, about the crossover temperature, and also about the Kauzman paradox [4] can thus be revealed, as the system changes its structure as it cools down below the crossover temperature and under T_g, as the particles generating the voids and associated with the higher amplitudes of motion disappear.

The limiting values of block time characteristic

For the time dependence limits for the fastest time interval of retardation we use the time interval calculated from the sound velocity, which for solid blocks is about 10^5–10^6 cm s^{-1}, and from the minimal length of acoustic waves, which are determined by the mesh size $\Delta r^*_{0,n}$. Thus we get: $1/\nu_{max} \cong \tau_{min}$ and $v_{sound} = \lambda_{min}\nu_{max}$, where $\lambda_{min} \approx 2\Delta r^*_{0,n}$.

Substituting from the estimate of values outlined above we get $\nu_{max} \cong 10^{13}$ s^{-1} for the maximum frequency in sample body and for the fastest time of material response in block $\tau_{min} \approx \nu_{max}^{-1} = 10^{-13}$ s. (The estimate on the fastest bottom well displacement based upon the experiment is quoted by Rossler [47], viz. $\tau_{min} = 3 \cdot 10^{-13}$ s.) For the longest time characteristic for the material we take the characteristic time connected with permanent displacement in series of elements inside of block space and bonded together through elastic force (Eqs (14), (15)).

The estimate on the size of blocks from the shear viscosity data

Numerous predictions regarding the size of the blocks are reported in literature by many authors [13, 50–56]. These predictions are based upon different experimental techniques. Focusing the attention now in a direction not yet used for the block size estimate, it will be tried in this study to provide the block size approximation, using the techniques of rheology. The answer is searched for two unknown parameters. The first represents the number of linear elements in block at which the blocks start to be interconnected in shear flow and start to interfere mutually producing a contribution to the elastic shear module response. A useful source of data, for the domains (block's) interactions, is the measurements of shear viscosity data obtained at zero velocity gradients, which have been known for about forty years for different structures of polymer melts with a variety of molecular mass values [57–59]. These data show one common feature in the dependence of shear viscosity on the number of monomer (acoustical [12]) units in chain X sequence. As is considered, as the first example, that the number 'X' is small and remains below a certain limit, $X \leq X_c$, where $X_c \approx 500$–625, and that the polymer melt is characterized by a constant and gradient-independent viscosity. In this particular case the module of shear elasticity is zero, as well as the first normal stress difference remains zero too. The macromolecules are smaller than the block size ($X \leq X_c$), and the blocks, if subjected to shear flow, do not exhibit any mutual interference. A different level of viscosity, which rises in linear dependence on X, characterizes each polymer at this particular case. However, at the point when the critical value X_c is reached in the polymer chains, there occur changes in the rheological properties. The block interconnections start to interfere through the overgrown size of macromolecules. For polymers with $X \geq X_c$ the melt viscosity in dependence on shear gradient starts to have the non-Newtonian character as the gradient grows and the first normal stress difference starts to be an important flow characteristic as well. This effect is usually explained in connection with the chain entanglements. The concept of entanglements was introduced originally base upon sketchy pictures [43, 60, 61] and as an evident phenomenon while the nature of couplings [60] was left as open, with the alternative to cooperative motions of molecular areas, which is also suited for the low molecular structures. The later case corresponds more closely to scheme presented in this study, which is also supported by findings of Achibat *et al.* [80, 81], reporting a relationship between the domains and the entanglements. The model presented attributes the property of inter-blocks bonding either to the entan-

glements (as the individual blocks start to be interwoven by polymer network) or to inflexible bonds of van der Waals type, or to the bonds of chemical nature. The inter-block bonding has a consequence in development of non-zero shear module. Although different polymers have different levels of viscosity or chain flexibility, different molecular mass, or exhibit different levels of normal stresses, the numerical value of X_c for blocks mechanical interference in shear flow has a universal character. Just quoting [59], for polystyrene X_c=600, for poly(vinyl acetate) X_c=600, for polyisobutylene X_c=500, for polydimethylsiloxane X_c=625. If the level of critical interconnection is reached in linear sequence for polymers, the blocks are inter-bonded and exhibit the shear elasticity represented by shear modulus or by the first normal stress difference. Such elasticity created by flexible macromolecules is entropy related. (This type of interconnection has a 'long distance character' relatively to the block size, and one macromolecule can 'over-bridge' several blocks too). In contrast to blocks connected by flexible macromolecules, the blocks can also be interconnected by inflexible chemical bonds. This is the case for the low molecular mass substances under the crossover temperature. The blocks connected by inflexible bonds cannot be stretched to higher deformations and have to break up as the temperature is increased above T_{cr}. The inflexible blocks interconnection reflects itself into the internal energy related shear module contribution under the T_{cr}. (This is valid for the block's contacts for the polymers under T_{cr} temperature too).

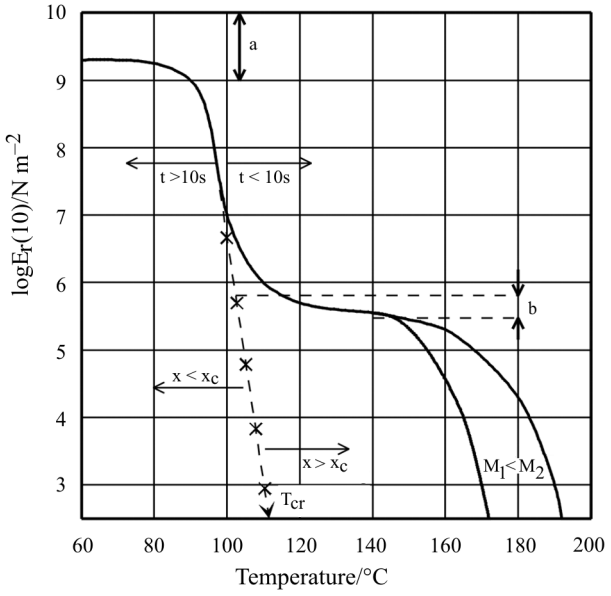

Fig. 5 The typical picture of relaxation module behavior of polymer. The sample is undergoing the temperature and molecular mass change. (According to Tobolsky [62] and Alkonis [63].) The elongation relaxation modulus of polystyrene, for two different molecular masses $M_w = M_1 \leq M_2$ as a function of temperature. The relaxation experiment is performed for a time of 10 s. The area 'a' stands for glassy zone and 'b' is the rubber-like zone [60, 61]

The parameter left to be determined is the crossover temperature itself. For these purposes the measurements of the dependence of shear relaxation module on temperature in area of main phase transition can provide this information [62, 63] (Fig. 5). For the reasons of clarity of explanations in text, some data of Schultz [59], Alkonis [63] and Tobolsky [62] were presented to show the idea behind the text more clearly. The crossover temperature T_{cr} (Fig. 5) is determined on the basis of the shear elasticity of internal energy related relaxation module. The value X_c is determined on the basis of the zero gradient viscosity curves. At this level of internal connection the blocks start to interfere in flow.

At the temperature T_{cr} the characteristic domain size can be estimated and for the lower temperatures $T \leq T_{cr}$, the part of force responding to external deformation has internal energy related component ($f_{INT} \neq 0$). Taking the size of one oscillator unit in interconnection sequence from the polarizability values [64, 65], for the interconnection number of X_c=600, the characteristic size of a domain of about 6 nm^3 (for the molecules of most typical size of pentane) can be obtained. For the linear dimension of a domain $6^{1/3}$=1.81 nm can be obtained. This seems to be in good agreement with the published values [13, 50–56] obtained by different experimental techniques. As the polarizability of molecules is simple additive properties of individual atomic polarizabilities, the domain size can be easily estimated, from the polarizabilities values of individual monomer unit and from the X_c values, as the Table 1 hints.

The spectra characteristic of the block

For the particles forming the block structures, in addition to the motion in ξ coordinate, which does not lead to linear particles diffusive displacements, an additional motion connected with $r_{0,n}$ displacements can be superimposed on the movements of particles. Besides the potential valley deformation the additional degree of freedom, if added to the particle movements, will bring by itself the increment in specific heat capacity c_p.

For the differentially small changes in bottom position $\delta r_{0,n}$ (Eq. 5), the coordinated changes of particles positions, $...r_{0,(n-1)}\ldots r_{0,(n+1)}$, $r_{0,(n+2)}\ldots\ldots r_{0,(n+k)}$ in the vicinity of semi-evaporated participle are needed as the precondition for permanent displacement of the n^{th} particle.

Table 1 Calculated domains size from the polarizabilities of acoustical units

The type of polymer	Estimate on polarizability of acoustical segment /Å^3	Domain size/nm for X_c=600
polystyrene	11.6	1.90
polyisobutylene	7.2	1.62
polybutadiene	6.4	1.55
polyvinyl acetate	8.0	1.68
polymethyl methacrylate	9.8	1.95
SiO_2	6.7	1.59
GeO_2	7.6	1.65
B_2O_3	4.4	2.05
As_2S_3	17.3	2.18
glycerol	8.6	1.72
pentane	10.0	1.81

$$\delta r_{0,n}(t) = \overline{f}(\delta_{0,(n-l)}(t)....\delta r_{0,(n+1)}(t), \delta r_{0,(n+2)}(t),.....\delta r_{0,(n+k)}(t) \quad (9)$$

The $\overline{f}$ stands for functional dependence and is taken as an unknown function of time t associated with material characteristic series of discrete retardation times. The actual positions of $r_{0,n}$, $r_{0,(n+1)}$ etc. does not enter into the mathematical formulation. The individual oscillators can be placed consecutively, in the space of sample, touching each other in form of necklace (Fig. 6). The mathematical formula will involve the particle consecutive order in chain time response and also the direction and size of deviations from equilibrium positions $\Delta r_{0,n}$, $\Delta r_{0,(n+1)}$, etc.

In simplistic view of interconnections for one line of particles connected in the form of an elastic necklace such as shown in Fig. 6 we get:

$$m_n \frac{d^2\Delta r_{0,n}}{dt^2} = k_e(\Delta r_{n,+1} - \Delta r_{0,n}) - k_e(\Delta r_{0,n} - \Delta r_{0,n-1}) + F_{ext} \quad (10)$$

Through extension of Eq. (10) inside of block we get:

$$m_n \frac{d^2\Delta r_{0,n}}{dt^2} = k_e(\Delta r_{0,n+1} + \Delta r_{0,n-l} - 2\Delta r_{0,n}) + f_{0n}^{Fr}\frac{\delta\Delta r_{0,n}}{\delta t} + F'_{ext} \quad (11)$$

where F_{ext} represents the external force acting on the particle through the particles localized in its vicinity. The simplest form of interconnections of elements, without branching or bridging is considered. The term F_{ext} can involve the effects of local friction force f_{0n}^{Fr}

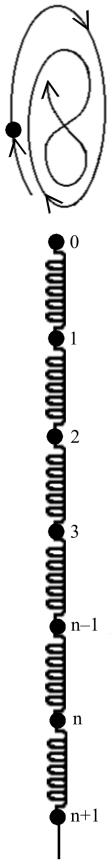

Fig. 6 A detail of Fig. 1. The individual particles in necklace are numbered according to their positions separating them from the non-linear particle stress perturbation shown schematically above of particle '0'

acting on each element $f_{0n}^{Fr}\frac{\delta\Delta r_{0,n}}{\delta t}$ expressed separately as shown in Eq. (11). The term F'_{ext} represents the interaction of non-linear oscillator (the semi-evaporated particle), acting on the ends of chain (point '0' in Fig. 6), by which the individual blocks segments are displaced in time. The non-linear oscillator of semi-evaporated particle acts as the local stress perturbation source on the necklace of elastically connected masses. The blocks play the role of the sidewalls, and from mathematical point of view, they act as the source of exact time response of material. For the case of F_{ext}=0 we get a homogeneous equation as a source for the calculation of vibration modes. These modes give the evidence about the actual distribution of resonance frequencies and time responses of material. The shifts in $\Delta r_{0,n}$ can be considered in any direction inside of sample.

$$m_n \frac{d^2\Delta r_{0,n}}{dt^2} = k_e(\Delta r_{0,n+1} + \Delta r_{0,n-l} - 2\Delta r_{0,n}) \quad (12)$$

Equations (10–12) have many classical solutions for many options of F_{ext} and are solved in connection with many different topics of engineering or scientific applications [18, 27, 43]. The typical solution to homogeneous Eq. (12) of relaxing block consists of series of resonance frequencies ω_n,

$$\omega_n^2 = \left(\frac{4k_e}{m_n}\right)\sin^2\left(\frac{n\pi}{2(N+1)}\right) \qquad (13)$$
$$n = 1,\ 2,\ 3,\ldots..\ N$$

and leads to the time response of blocks characterized by series of relaxation or retardation times (for creep related experiments) of interconnected elements [18, 43].

(The solutions of Eqs (11)–(13) are given in Appendix A and B. Please note also that for $\sin^2\left(\frac{n\pi}{2(N+1)}\right)$ and $n \le \frac{N}{2}$ the argument of $\sin^2\left(\frac{n\pi}{2N}\right) \approx \text{const.}\frac{n^2}{4N^2}$ is valid.)

Solving Eq. (13) means finding the resonance frequencies ω_n, which determine the mechanical characteristics of the block. The block is invariably a linear system, and the times of block response are given through simple arithmetic multiplication if constant local friction is considered.

$$\tau_n = \frac{f_{0,n}^{Fr}}{\omega_n^2 m_n} \qquad (14)$$

and for the constant frictions and masses of each oscillator inside of block $f_{0,n}^{Fr} / m_n = \text{const}' = \tau_1$, we get:

$$\tau_1 \cong \frac{\tau_n}{n^2} \qquad (15)$$

For the sequence of resonance modes in the sense of Eq. (12) the matrix $\Omega = \begin{pmatrix} 1 & -2 & 1 & \\ & 1 & -2 & 1 \\ & \ldots\ etc. & \ldots & \end{pmatrix}$ of Eq. (12) plays the crucial role in the separations of retardation times and in the separation of resonant frequencies of ω_n. From Eq. (11) for the case of the n^{th} element we get $\omega_n^2 = \frac{k_e}{m_n} = \frac{f_{0,n}^{Fr}}{m_n \tau_n}$.

Taking the ratio between the elasticity and friction for each oscillator in block as the same $k_e / f_{0,n}^{Fr} = \text{const} = \tau_1^{-1}$, Eq. (12) gives very simplified spectra distribution $\tau_n = \tau_1 n^2$. It can be seen that the higher retardation times are formed in blocks spaces through growing sequence of interconnected elements and not through variation of local friction or local elasticity. The friction force $f_{0,n}^{Fr}$ or the external forces F'_{ext}, F_{ext} do not influence the separation of individual material time responses either.

The individual retardation times covering the motions inside of blocks, are mutually interdependent through Eq. (15) (Figs 7, 8). The time for total block displacement is thus proportional to N^2 while the friction force for the block movement, which characterizes the shear viscosity of sample, remains proportional to N only if the total block friction is defined as $\sum_{i=1}^{N} f_{0n}\frac{d\Delta r_{0,n}}{dt}$. It can be assumed that the friction coefficients $f_{0,n}$ of 'beads' inside the solid 'icebergs' vary only mildly with temperature changes. However, it is expected that the number N increase smoothly with decreasing temperature. At the crossover temperature the inter-chain branching start to appear. The knots and bridges between the chains characterizing the structure, affect the relaxation times in different way from the viscosity, making the chain sequences shorter. For example if two necklaces are connected together, then the viscosity rises by factor of two. The rise in maximal relaxation time will depend on the way how the interconnection is made, leaving the maximum increase only for the head-tail interconnection type. (The last reports on relaxation time and viscosity measurements [13] state that while the viscosity increases with slope of 3.4 with average molecular mass $M_w^{3.4}$, the increase in maximal relaxation time is less dramatic ($M_w^{3^\circ}$) [66].

The 'alpha' and 'beta slow' processes – the mechanical shelters for shear elasticity components

The retardation time τ_1 is thus the starting point in a sequence through which the longer retardation time τ_n can be created. The longest retardation time τ_N should grow with decreasing temperature and reflect the approximation for the level of interconnections in linear elements of block size.

The term τ_N stands for the time necessary for displacement of a block as a whole. The shortest retardation time will reflect the fastest response of bottom of potential valley by differentially small displacements of $\Delta r_{0,n}$. The fastest displacement will involve only the acoustical units in shortest vicinity of the particle considered. Because the acoustical units usually contain few atoms and are approximately of monomer size [12], the shortest relaxation time is expected to represent connection of about 20–100 atoms and to be in the vicinity of the so-called β_{fast} relaxation process [49]. One 'bead' in necklace pictured in Fig. 6 will be involved in the friction force of many molecules forming the first level of coordinated motion in the closest neighborhood of the particle displaced. (This will provide the relaxation time in the vicinity of the so-called β_{fast} relaxation process, which is reported [49, 67] to be about 3.0×10^{-13} s). It can be seen in Figs

7 and 8 that for the so-called α (line 'A') relaxation process the interconnection level reaches infinity as soon as the temperature decrease starts to approach the T_g temperature and the infinite elastic network is developed. The so-called β_{slow} process (lines 'B, C, D') is different because the parameter N for these processes cannot reach the infinite interconnection level as the temperature decreases. Searching the τ_N at the crossover temperature for 600 elements we get $\tau_N(T=T_{cr})=\tau_1\cdot 600^2=3.0\cdot 10^{-13}\cdot 600^2\approx 1.08\cdot 10^{-7}$ s. Rossler [49] experimentally confirmed such characteristic time level at the crossover temperature. Below the T_{cr} temperature the term $\tau_\alpha\rightarrow\infty$, which means, that

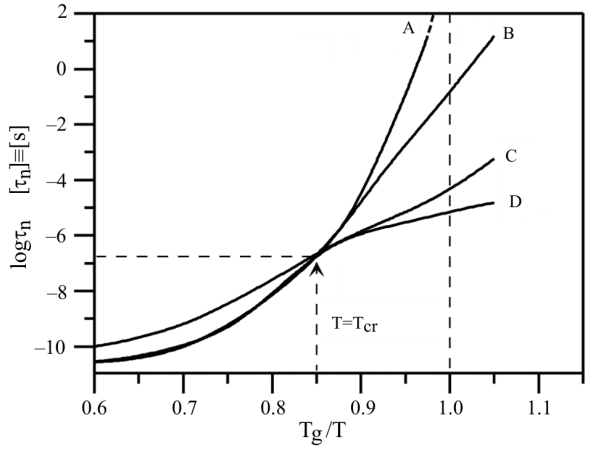

Fig. 7 The logarithms of characteristic relaxation times determined by Rossler [49] for variety of organic and inorganic materials. The graphs are testing the sequence shown in Eqs (14, 15). Rossler's relaxation times τ are taken for the limiting variable interconnection number N. In our model, $\tau_1=3\cdot 10^{-13}$ s and $\tau_{600}=10^{-7}$ s according to Rossler [49] and according to Eq. (15). At $T=T_{cr}$ we take the N value equal to 600

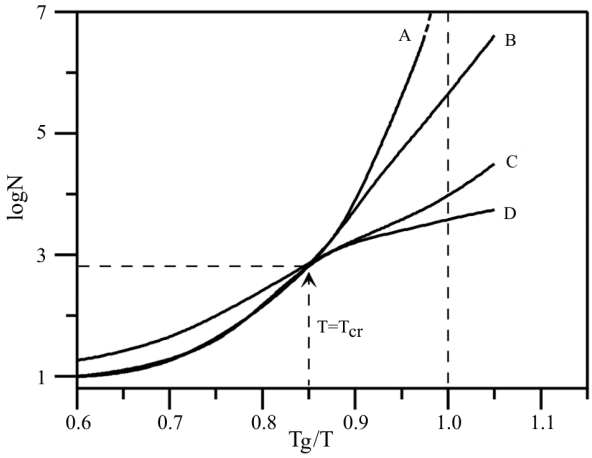

Fig. 8 The numbers of linear interconnections N for variable relative temperatures obtained from Eq. (15). The limited interconnection level for β_{slow} processes (curves B, C, D), below T_g are clearly visible

the sample elasticity is mainly connected to the particles associated with α process as the elastically interconnected network covering the space of a whole sample is formed. On the other hand, the particles connected with β_{slow} process are apparently anchored in space differently, being ultimately bound with very high viscosity coefficient rather than with purely elastic response to external shear deformation. It can be stated that the β_{slow} processes are connected with the 'loosely anchored' or floating parts of a network structure.

Because the area between the T_{cr} and T_g is connected with sharp increase in shear modulus, it can be said that the β_{slow} processes are shear-module-insensitive. Therefore, the β_{slow} processes appear to be localized in sample in different, mechanically sheltered areas, which certainly transport the shear component of stress in a way different from what the α process does. Because the number of interconnected elements forming the β_{slow} process does not reach infinity (which is the precondition for the formation of elastic solid phase with the infinite relaxation time), the elastic solid phase formation seems to be determined by the α process.

The views presented in this paper are more closely approaching the description of β process presented in early theories [71–76] of Eisenberg [77, 78], Heijboer [74–76] and Bueche [43] which has been taken as well proofed by experiment and which contradict the recent theories which are involving all particles of the system participating in the β slow motions [69]. The theories of plasticizers [79] suggest also the structural heterogeneity and give example of materials for which the islands of mobility can be hardly excluded. (On the other hand, in the case of glycerol, the β_{slow} process is not present). The other explanation for the β_{slow} processes is connecting them with changes in coordinates displacements not directly connected with external shear deformation (the perpendicular rotation of two different parts of polymer chains around two perpendicular axes has been described already by Bueche [43] in his discussion of substance of α and β_{slow} processes.)

These studies are the subject of our various interdisciplinary projects and are the continuation of our previous and recent interrelated discussions published in different sources such as papers [16, 82–83] or books [84, 85].

Conclusions

The estimate on the size of domain at crossover temperature has been provided based upon the rheological data of viscosity at zero gradients.

The crossover temperature has been estimated from the relaxation module data. The crossover temperature is connected to first appearance of internal energy related shear module.

The irregular structure of amorphous phase has been explained through the existence of non-deterministic oscillators, which exist in liquid phase. The disappearance of these particles under the T_g and the non-predictability of end points of their positions in phase space coordinates gives rise to the existence of irregular structure of amorphous phase.

The non-linear oscillators have also an abnormal coefficient of thermal expansion and the amorphous liquid is thus structurally different from the amorphous solids, which casts some light into the explanations regarding the Kauzman paradox [4]. The Kauzman paradox is based on extrapolation and does not take into account the fact, that the liquid is a mechanically heterogeneous substance in which the heterogeneity is partially removed as the temperature goes down below T_g, and the highly non-linear oscillators disappear. The liquid phase is structurally different from the solid in mechanical sense, viz. by the appearance and disappearance of highly mobile, diffusive, non-linear oscillators.

The α and β_{slow} processes seem to have a common origin in the β_{fast} process. The α process differs from the β_{slow} process in numbers of interconnected elements, which increase for the α process to infinity as the sample solidifies. The β_{slow} process does not possess this property and apparently is not 'fully' contributing to the shear elasticity level. Being localized inside of blocks, the β_{slow} process is insensitive to the inter-blocks bridging which gives rise to shear module and as such, the β_{slow} process need not to be present in some materials, at the point of formation of glassy state. The characteristic vibration frequencies of linear domains localized outside the non-linear areas provide the source for discrete characteristic time spectra. The experimental data supporting the double character of vibration and double values for amplitude sizes have been recently brought forward by Medick *et al*. [46] and by previous work of Rossler *et al*. [68–70].

Appendix A: Differential displacements of particles in block ruled by wave equation

The solution of Eqs (10, 11) in the form of Eqs (13–15) has many interesting features, and some of them should be mentioned. The first interesting feature seems to be the fact that Eqs (10–12), relating the individual bottom well displacements $\Delta r_{0,n}$ for many (n) particles do not have to depend on the actual bottom wells positions of $r_{0,n}$ of interconnected particles. As a special solution, Eqs (10–12) can represent the wave equation for vibration modes of elastic rod, or the motion of spring with the equally distributed masses m_n per length $l=(N+1)\alpha=(N+1)\delta x\ldots$ where α is a distance between subsequently connected masses $m_{n-1}=m_n=\ =m_{n+1}=m\delta x\ldots$ etc.

Except for the variability of shape of irregular block, the elastic rod seems to be the geometrically nearest object resembling the block structure. If choosing the following substitution in Eqs (10–12) for the $k_e=T_e/\alpha$; $\rho\,\mathrm{d}x=m_n$ where ρ is a bar (spring) density, then Eqs (12–14) take the form of wave equation for $\underline{F}_{ext}=0$.

$$m_n\frac{\mathrm{d}^2\Delta r_{0,n}}{\mathrm{d}t^2}=k_e(\Delta r_{0,n+1}+\Delta r_{0,n-1}-2\Delta r_{0,n}) \tag{16}$$

$$\begin{aligned}\frac{\mathrm{d}^2\Delta r_{0,n}}{\mathrm{d}t^2}&=\frac{T_e}{m}\left(\frac{\Delta r_{0,n+1}-2r_{0,n}+r_{0,n-1}}{\delta x}\right)=\\ &=\frac{T_e}{m}\left(\frac{\Delta r_{0,n+1}-\Delta r_{0,n}}{\delta x}-\frac{\Delta r_{0,n}-\Delta r_{0,n-1}}{\delta x}\right)=\\ &=\frac{T_e}{m}\left(\frac{\delta\Delta r_0}{\delta x}\right)_{n+1}-\left(\frac{\delta\Delta r_0}{\delta x}\right)_n\end{aligned} \tag{17}$$

$$\frac{\mathrm{d}^2\Delta r_0}{\mathrm{d}t^2}=\frac{T_e}{\rho}\frac{\mathrm{d}^2\Delta r_0}{\mathrm{d}x^2} \tag{18}$$

The connection of difference equation to the wave equation opens further possibilities connected to elasticity and fracture theories.

Appendix B: Solution of difference equation in form of Eqs (12)

The solution of Eqs (12) can be searched in form: $\Delta r_0\propto e^{j(\omega t-\bar{k}x)}$ where $\bar{k}$ is a wave vector.

$$\bar{k}=\left(\frac{\rho}{T_e}\right)^{\frac{1}{2}}\omega \tag{19}$$

In discrete form for the n^{th} particle we get: $\Delta r_{0,n}=A_n e^{j(\omega t-\bar{k}x)}=A_n e^{j(\omega t-\bar{k}an)}$ since $x=na$.

Substituting these expressions into Eq. (14) provides:

$$\begin{aligned}\omega_n^2 m_n&=\frac{T_e}{a}(e^{j\bar{k}a}+e^{-j\bar{k}a}-2)=\\ &=\frac{T_e}{a}(e^{j\bar{k}\frac{a}{2}}-e^{-j\bar{k}\frac{a}{2}})^2=-\frac{4T_e}{a}\sin^2\frac{\bar{k}a}{2}\end{aligned} \tag{20}$$

Substituting from boundary conditions, i.e. that the oscillators 'out of sample' with index $n=0$ and index $n=N+1$ can be associated with zero amplitudes $A_n=0$, we get the convenient substitution:

$$\frac{\bar{k}a}{2}=\frac{n\pi}{2(N+1)} \tag{21}$$

$$\omega_n^2=\frac{2T_e}{m_n a}\left(1-\cos\frac{n\pi}{N+1}\right)=\frac{4T_e}{ma}\sin^2\frac{n\pi}{2(N+1)} \tag{22}$$

Acknowledgements

The authors are grateful for the financial support from the research project No. 0021627501 (Ministry of Education, Czech Republic) and to Dr. J. Bartoš from Slovak Academy of Sciences, Bratislava.

References

1 H. E. Stanley, Introduction to Phase Transitions and Critical Phenomena, Oxford University Press, New York 1971.
2 J. O. Hirschfelder, C. F. Curtiss and R. B. Bird, Molecular Theory of Gases and Liquids, J. Wiley, New York 1954, pp. 122, 291.
3 W. Gotze and L. Sjogren, Rep. Prog. Phys., 55 (1992) 241.
4 W. Kauzmann, Chem. Rev., 43 (1948) 219.
5 M. Cohen and D. Turnbull, J. Chem. Phys., 31 (1959) 1164.
6 D. Turnbull and M. H. Cohen, J. Chem. Phys., 34 (1961) 120.
7 D. Turnbull, in: Thomas J. Hughel, Liquids: Structure, Properties and Solid Interaction, Proceedings of Symposium, Elsevier, Amsterdam 1965, pp. 6–24.
8 D. Turnbull, Contemp. Phys., 10 (1969) 473.
9 G. S. Grest and M. H. Cohen, Phys. Rev., 21 (1980) 4113.
10 M. H. Cohen and G. S. Grest, Phys. Rev., B20 (1979) 1077.
11 G. S. Grest and M. H. Cohen, in: I. Prigogine and S. T. Rice, Advances in Chem. Phys., Vol. XLVII, J. Wiley, New York 1981, pp. 455–525.
12 A. Heuer and H. W. Spiess, J. Non-Cryst Solids, 176 (1994) 294.
13 E. Donth, The Glass Transition, Relaxation Dynamics in Liquids and Disordered Materials, Springer Verlag, Berlin, Heidelberg 2001.
14 A. Einstein, Investigation on the theory of the Brownian Movement, Ed. R. Furth, Dover Publications, Inc., New York, N.Y. 1956.
15 B. Hlaváček, V. Křesálek and J. Souček, J. Chem. Phys., 107 (1997) 4658.
16 B. Hlaváček, J. Šesták and J. Mareš, J. Therm. Anal. Cal., 67 (2002) 239.
17 M. I. Rabinowitz, A. B. Ezersky and P. D. Weidman, The Dynamics of Patterns, World Sci. Publ., Singapore 2000, pp. 239–279.
18 H. J. Paine, The Physics of Vibrations and Waves, J. Wiley, New York 1997.
19 U. Ueda, New Approaches to Non-linear Dynamics. S.I.A.M., Philadelphia 1980.
20 M. Tabor, Chaos and Integrability in Non-linear Dynamics, John Wiley, New York 1989.
21 I. Prigogine and I. Stengers, Order out of Chaos, Bantam Books, New York 1984.
22 D. Kondempundi and I. Prigogine, Modern Thermodynamics, J. Wiley, New York 1998, pp. 409–452.
23 O. E. Rössler, Phys. Lett., 57A (1976) 397.
24 E. N. Lorenz, J. Atm., Sci. 20 (1963) 130.
25 A. Tockstein, Chemické listy, 81 (1987) 569.
26 P. G. DeBenedeti, Metastable Liquids, Princeton Univ. Press, Princeton, New Jersey 1996.
27 J. Frenkel, Kinetic Theory of Liquids, Dover Publ. Inc., New Jersey 1955, p.12.
28 V. Velikov, S. Borick and C. A. Angel, J. Phys. Chem., B106 (2002) 1069.
29 W. Xu, E. I. Cooper and C. A. Angel, J. Phys. Chem., B107 (2003) 6170.
30 H. J. Parkhurst Jr. and J. Jonas, J. Chem. Phys., 63 (1975) 2699.
31 R. Zwanzig, J. Chem. Phys., 79 (1983) 4507.
32 U. Buchenau and M. Zorn, Europhys. Lett., 18 (1993) 523.
33 A. Eisenstein and N. S. Gingrich, Phys. Rev., 62 (1942) 261.
34 J. Bartoš, Colloid Polym. Sci., 274 (1996) 14.
35 J. Bartoš, P. Bandžuch, O. Šauša, K. Krištiaková, J. Krištiak, T. Kanaya and W. Jenniger, Macromolecules, 30 (1997) 6906.
36 Y. C. Jean, Microchem. J., 42 (1990) 72.
37 Y. C. Jean, Macromolecules, 29 (1996) 5756.
38 Y. C. Jean, Q. Deng and T. T. Nguyen, Macromolecules, 28 (1995) 8840.
39 G. P. Johari, J. Chem. Phys., 116 (2002) 2043.
40 G. P. Johari, J. Chem. Phys., 112 (2000) 10957.
41 R. E. Powell, W. E. Roseveare and H. Eyring, Ind. Eng. Chem., 33 (1941) 430.
42 S. Glasstone, K. J. Laidler and H. Eyring, The Theory of Rate Processes, McGraw-Hill Book, New York–London 1941.
43 F. Bueche, Physical Properties of Polymers, Interscience, New York–London 1962, p.106.
44 M. Vogel and E. Rossler, J. Phys. Chem., B104 (2000) 4285.
45 G. P. Johari, Phil. Mag., 81 (2001) 1935.
46 P. Medick, M.Vogel and E. Rossler, J. Magn. Reson., 159 (2002) 126.
47 C. Tschirwitz, S. Benkhof, T. Blochowitz and E. Rossler, J. Chem. Phys., 117 (2002) 6281.
48 S. Adichtchev, T. Blochowitz, C. Gainaru, V. N. Novikov, E. A. Rossler and C. Tschirwitz, J. Phys. Condens. Matter, 15 (2003) 835.
49 E. Rossler, Phys. Rev., 69 (1992) 1595.
50 E. Donth, J. Non-Cryst. Solids, 53 (1982) 325.
51 T. Dollase, R. Graf, A. Heuer and H. W. Spiess, Macromolecules, 34 (2001) 298.
52 J. Bartoš, O. Šauša, J. Krištak, T. Blochowity and E. Rossler, J. Phys. Condens. Matter, 13 (2001) 11473.
53 M. Beiner, H. Huth and K. Schroter, J. Non-Cryst. Solids, 279 (2001) 126.
54 E. Hempel, M. Beiner, T. Renner and E. Donth, Acta Polymer., 47 (1996) 525.
55 U. Mohanty, G. Diezeman and I. Oppenheim, J. Phys. Condens. Matter, 12 (2000) 6431.
56 S. A. Reinsberg, X. H. Qiu, M. Wilhelm, H. W. Spiess and M. D. Ediger, J. Chem. Phys., 114 (2001) 7299.
57 V. R. Allen and T. G. Fox, J. Chem. Phys., 41 (1964) 337.
58 T. G. Fox and V. R. Allen, J. Chem. Phys., 41 (1964) 344.
59 J. Schulz, Polymer Material Science, Prentice-Hall, Englewood Cliffs, New Jersey 1974, p. 337.
60 J. D. Ferry, Viscoelastic Properties of Polymers, Wiley, New York–London 1961, p. 225.
61 F. Bueche, J. Chem. Phys., 20 (1956) 599.

62 A. V. Tobolsky, Properties and Structure of Polymers, J. Wiley, New York 1960 p. 75.
63 J. J. Aklonis, W. J. MacKnight and M. Shen, Introduction to Polymer Viscoelasticity, Wiley-Interscience, New York– London 1972, p. 42.
64 B. Hlaváček, E. Černošková, L. Prokůpek and M. Večeřa, Thermochim. Acta, 280/281 (1996) 417.
65 D. R. Lide, Handbook of Chemistry and Physics, 82nd Ed., 10, CRC Press LLC, Washington D. C. 2002, pp. 160–174.
66 M. Doi and S. F. Edwards, Theory of Polymer Dynamics, Clarendon Press, Oxford 1986.
67 M. Vogel and E. Rossler, J. Phys. Chem., B104 (2000) 4285.
68 J. Wiederich, N. V. Surovtsev and E. Rossler, J. Chem. Phys., 113 (2000) 1143.
69 M. Vogel and E. Rossler, J. Chem. Phys., 114 (2001) 5802.
70 M. Vogel and E. Rossler, J. Chem. Phys., 115 (2001) 10883.
71 E. Jeckel and H. U. Herwig, Kolloid Z., 148 (1956) 57.
72 R. F. Boyer, J. Macromol. Sci. Phys., B7 (1973) 487.
73 R. F. Boyer, J. Polym. Sci., Polym. Symp., 50 (1975) 189.
74 J. Heijboer, Kolloid Z., 148 (1956) 36.
75 J. Heijboer, Kolloid Z., 171 (1960) 7.
76 J. Heijboer, Ph.D. Thesis, University of Leiden, 1972.
77 B. Cayrol, A. Eisenberg, J. F. Harrod and P. Rocaniere, Macromolecules, 5 (1972) 676.
78 A. Eisenberg, 'The Glassy State' in: J. E. Mark, A. Eisenberg, W. W. Graessley, L. Mandelkern, E. T. Samulski, J. L. Koenig and G. D. Wignall, Physical Properties of Polymers, Amer. Chem. Soc., Washington D.C. 1993, pp. 61–97.
79 H. E. Bair, Thermal Analyses of Additives in Polymers, in: E. A. Turi, Thermal Characteristic of Polymeric Materials, Vol. 2, J. Wiley, Academic Press, New York 1997, pp. 2263–2412.
80 T. Achibat, A. Boukenter, E. Duval, G. Lorentz and S. Etienne, J. Chem. Phys., 95 (1991) 2949.
81 E. Duval, A. Boukenter and T. Achibat, J. Phys. Condens. Matter, 2 (1990) 10227.
82 J. Šesták: 'Trends and boundary aspects of non-traditionally applied science of heat' presented at the seminary 'Present and future of JTAC' (Budapest, 2003), abstracted in: J. Therm. Anal. Cal., 75 (2004) 1006.
83 J. J. Mareš and J. Šesták, J. Therm. Anal. Cal., (2005) submitted
84 J. Šesták, book: 'Heat, Thermal Analysis and Society', Nucleus, Hradec Králove 2004.
85 Z. Chvoj, J. Šesták and A. Tříska, book 'Kinetic Phase Diagrams: non-equilibrium phase transitions', Elsevier, Amsterdam 1991.